

## Structure of Cubic Aluminate Sodalite $\text{Ca}_8[\text{Al}_{12}\text{O}_{24}](\text{WO}_4)_2$ in Comparison with its Orthorhombic Phase and with Cubic $\text{Sr}_8[\text{Al}_{12}\text{O}_{24}](\text{CrO}_4)_2$

BY W. DEPMEIER\*

*Institut für Kristallographie, Universität Karlsruhe (TH), D-7500 Karlsruhe, Federal Republic of Germany*

(Received 8 June 1987; accepted 26 November 1987)

### Abstract

Hexaaluminium tetracalcium dodecaoxide tungstate,  $M_r = 1524.1$ , cubic,  $I\bar{4}3m$ ,  $a = 9.300(4) \text{ \AA}$ ,  $V = 804(1) \text{ \AA}^3$ ,  $Z = 1$ ,  $D_x = 3.15 \text{ Mg m}^{-3}$ ,  $\lambda(\text{Mo } K\alpha) = 0.7107 \text{ \AA}$ ,  $\mu(\text{Mo } K\alpha) = 8.99 \text{ mm}^{-1}$ ,  $F(000) = 720$ ,  $656 < T < 783 \text{ K}$ , final  $R = 0.040$  for 139 unique reflections. The essential feature of cubic  $\text{Ca}_8[\text{Al}_{12}\text{O}_{24}](\text{WO}_4)_2$  is the orientational disorder of the  $\text{WO}_4$  anions. This is transmitted as positional disorder to the framework, as well as to the Ca cations. The refined positions of cubic  $\text{Ca}_8[\text{Al}_{12}\text{O}_{24}](\text{WO}_4)_2$  match the *average* positions of its orthorhombic phase very well. This suggests that the static, translationally periodic atomic displacements of the orthorhombic phase become non-periodic – supposedly dynamic – in the cubic phase. The principal structural characteristics of the framework, namely tetrahedron distortion and partial collapse, are common to both phases of  $\text{Ca}_8[\text{Al}_{12}\text{O}_{24}](\text{WO}_4)_2$ . With the exception of partial collapse, the cubic phase of  $\text{Sr}_8[\text{Al}_{12}\text{O}_{24}](\text{CrO}_4)_2$  corresponds to that of the title compound.

### Introduction

Aluminate sodalites of general composition  $M_8[\text{Al}_{12}\text{O}_{24}](\text{XO}_4)_2$ , with  $M = \text{Ca}, \text{Sr}, \dots$  and  $X = \text{S}, \text{Cr}, \text{Mo}, \text{W}, \dots$ , are interesting for several reasons, one being the occurrence of ferroic phase transitions, from cubic at high temperatures to non-cubic at lower temperatures, in all known pure members of the series. The title compound (henceforth CAW) was the first aluminate sodalite for which detailed structural information became available [room-temperature phase, RT-CAW (Depmeier, 1984*a*; D1 hereafter)]. In particular, it could be shown that the non-cubic symmetry of RT-CAW and its complicated superstructure were connected with the ordered arrangement of the tetrahedral  $\text{WO}_4$  cage anions that have orientations in which their threefold axes do not coincide with those of the sodalite framework (so-called 'tetragonal orientation'). Starting from the results of investigations on mixed crystal systems it was proposed (Setter & Depmeier,

1984) that the cubic phases of all aluminate sodalites were connected with disorder of the  $\text{XO}_4$  anions over the various symmetrically equivalent 'tetragonal' orientation states. The phase transitions to non-cubic phases were then supposed to be triggered by ordering processes involving primarily these groups. The correctness of the first part of this assumption could be verified, in at least one case, by the refinement of the cubic phase of  $\text{Sr}_8[\text{Al}_{12}\text{O}_{24}](\text{CrO}_4)_2$  [SACR (Depmeier, Schmid, Setter & Werk, 1987; DSSW hereafter)].

For several years CAW has been known to undergo two structural phase transitions at 614 and 656 K (Depmeier, 1979); however, no definite structural information on the two high-temperature phases is yet available. The present study covered this temperature range and it can now be confirmed that the phase stable above 656 K is indeed cubic. For the intermediate phase only limited information could be obtained. Therefore, this will not be published until sound results of forthcoming experiments, concentrating on this phase, are available.

In some respects cubic CAW is quite similar to cubic SACR. However, the structural details – in particular the fact that CAW is partially collapsed – make it sufficiently distinct from SACR that a detailed comparison of the two phases is appropriate. Furthermore, the structure of CAW is now known in two of its phases. It is certainly of general importance for our knowledge of all aluminate sodalites to discuss the difference between the two phases, as this can shed light on general features of the phase transitions occurring in this structural family.

For descriptions and discussions of the basic features of the cubic sodalite structure the reader is referred to the literature (*e.g.*, Hassan & Grundy, 1984; Koch & Hellner, 1981; Depmeier, 1984*b*, D2).

### Experimental

The crystal used in this study was grown and selected as described earlier (D1); it was approximately wedge-shaped, diameter 100  $\mu\text{m}$ ; a test of twinning at room temperature exhibited the same twin law and similar volume fractions as for the crystal used in D1; the crystal was mounted with a temperature-resistant

\* Present address: Institut für Mineralogie und Kristallographie, TU Berlin, D-1000 Berlin 12, Federal Republic of Germany.

Table 1. Fractional atomic coordinates and equivalent isotropic displacement parameters  $U_{eq}$  ( $\text{\AA}^2 \times 10^3$ ) for cubic CAW

E.s.d.'s are in parentheses,  $U_{eq} = \frac{1}{3}$  trace  $U$ . Averaged pseudocubic coordinates for the orthorhombic room-temperature phase of CAW (RT-CAW, D1) are given in square brackets, with the e.s.d.'s of the average in angled brackets. The last three columns contain the corresponding  $U_{eq}$  of cubic SACR (DSSW), the averaged  $U_{eq}$  for RT-CAW (with averaged e.s.d.'s) and the number of independent atoms of RT-CAW contributing to the averages.

Wyckoff notation	Site symmetry	Occupancy	x	y	z	$U_{eq}$ for cubic CAW	$U_{eq}$ for cubic SACR	Averaged $U_{eq}$ for RT-CAW	No. of independent atoms for RT-CAW
Al	12(d)	1.0	$\frac{1}{2}$	$\frac{1}{2}$	0	31 (1)	12 (1)	6 (1)	7
O	24(g)	1.0	[0.25 <1>] 0.1575 (6)	[0.50 <1>] 0.1575 (6)	[0.00 <1>] 0.4680 (8)	58 (3)	24 (1)	10 (1)	12
Ca	8(c)	1.0	[0.16 <2>] 0.2339 (5)	[0.16 <2>] 0.2339 (5)	[0.47 <2>] 0.2339 (5)	64 (1)	61 (1)	12 (2)	4
W	2(a)	1.0	[0.23 <2>] 0	[0.23 <2>] 0	[0.23 <2>] 0	57 (1)	47 (1)	12 (1)	1
O2	24(g)	$\frac{1}{2}$	[0.01223 (2)] 0.368 (3)	[-0.03281 (3)] 0.368 (3)	[0] 0.476 (6)	147 (15)*	115 (13)*	29 (5)	4
			[0.37 <3>]	[0.37 <3>]	[0.46 <2>]				

\* Isotropic  $U$  values.

Table 2. Important interatomic distances ( $\text{\AA}$ ) and angles ( $^\circ$ ) of cubic and orthorhombic CAW

The values given for orthorhombic CAW are averaged values of those given in D1. E.s.d.'s for cubic CAW are in parentheses. For the orthorhombic phase the e.s.d. of the mean value is given in angled brackets, the number of contributing items is also given. Last column: notations used in D2 for the description of the sodalite framework.

	Cubic CAW	Orthorhombic RT-CAW	No. of independent items in RT-CAW	Notations in D2
Al-O	4 × 1.725 (2)	1.74 (2)	24	$l$
O...O	2 × 2.989 (12)	3.01 (5)	14	$d_1$
	4 × 2.725 (2)	2.76 (6)	24	$d_2$
∠O-Al-O	2 × 120.2 (5)	120 (3)	14	$\alpha$
	4 × 104.4 (2)	105 (3)	24	$\alpha'$
∠Al-O-Al	144.8 (5)	142 (11)	12	$\gamma$
Al...Al	3.288 (1)	3.28 (9)	12	$u$
Tilt angle	11.5 (5)	13 (8)	12	$\phi$
Ca-O	3 × 2.398 (8)	2.39 (5)	12	
	3 × 2.856 (8)	2.9 (3)	12	
Ca-O2	3 × 2.75 (5)	2.39 (7)	5*	
	3 × 2.86 (5)			
W-O2	12 × 1.75 (4)	1.77 (2)	4	
O-O2	12 × 2.77 (4)	3.0 (1)	4*	

\* Shortest distances only.

silicone sealing cement on a modified (Anselment, 1986) Enraf-Nonius crystal heater; important deviations of real from nominal temperatures were observed; the cubic phase was identified by disappearance of all types of superstructure reflections of RT-CAW; twinning as observed at room temperature had also disappeared (for twinning by inversion, see below); nominal temperature for data collection 783 K, true temperature between 656 and 783 K; lattice parameters by least squares from centring 22 strong reflections,  $10 < 2\theta < 31^\circ$ . Data collection: Syntex R3 diffractometer, graphite monochromator; one octant only to avoid hardware collision problems ( $0 \leq h, k \leq 14$ ,  $-14 \leq l \leq 0$ );  $(\sin\theta/\lambda)_{\max} = 0.70 \text{ \AA}^{-1}$ ,  $\omega$  scans, scan width  $0.9^\circ$ , variable scan speed  $0.05\text{--}0.2^\circ \text{ s}^{-1}$ , background measured on both sides of the reflection, total background time = 0.5 times the time used for the peaks; three standards measured every 100 reflections showed a 5% fall-off over the measuring time, which was attributed to a slight movement of the crystal, data

corrected correspondingly; 700 reflections, 456 with  $I > 3\sigma(I)$ ; Lorentz and polarization corrections; no absorption correction,  $\mu R \approx 0.5$ ; 145 unique reflections after averaging,  $R_{\text{int}} = 0.04$ . Structure refinement: started with ideal coordinates for Ca, Al, framework O and W,  $\text{WO}_4\text{-O}$  atoms (O2 henceforth) from difference Fourier map; full-matrix least squares,  $\sum w(|F_o| - |F_c|)^2$  minimized,  $w = [\sigma^2(F_o) + 0.0001F_o^2]^{-1}$ ; scattering factors for neutral atoms,  $f'$  and  $f''$  from *International Tables for X-ray Crystallography* (1974); anisotropic atomic displacement parameters for Ca, Al, W and framework O, isotropic for O2;  $I\bar{4}3m$ , 139 unique reflections with  $F_o > 3\sigma(F_o)$ , 18 parameters including empirical extinction correction and an 'absolute configuration' parameter (Rogers, 1981), the latter refined to a value of 0.16 (0.11), indicating twinning by inversion; final  $R = 0.0396$ ,  $wR = 0.0358$ ; \* maximum shift/e.s.d. after final least-squares cycle 0.02, strongest peak in final difference Fourier map  $1.6 \text{ e \AA}^{-3}$  on W. All calculations performed with *SHELXTL* (Sheldrick, 1978) on a Nova 3 computer.

## Results and discussion

The final atomic positional and equivalent isotropic displacement parameters for cubic CAW are listed in Table 1. They are compared with the corresponding parameters for RT-CAW. Equivalent isotropic displacement parameters for SACR are also given. Table 2 lists important distances and angles for cubic CAW and RT-CAW. Note that the specifications for RT-CAW given in Tables 1 and 2 refer to the pseudocubic unit cell and are, in general, mean values of parameters which are non-equivalent under orthorhombic sym-

\* Lists of structure factors and anisotropic atomic displacement parameters have been deposited with the British Library Document Supply Centre as Supplementary Publication No. SUP 44613 (4 pp.). Copies may be obtained through The Executive Secretary, International Union of Crystallography, 5 Abbey Square, Chester CH1 2HU, England.

metry. These may vary considerably and, as a measure of the variance, the standard deviation of the respective mean value is given in angled brackets. The number of contributing items is also specified. The equivalent isotropic displacement parameters of symmetrically non-equivalent atoms of RT-CAW are very uniform and the error indication given in Table 1 is the mean e.s.d. of the least-squares procedure. The standard deviations of cubic CAW and cubic SACR are the usual ones and are given in parentheses.

In the case of cubic SACR (DSSW), we encountered insurmountable difficulties in determining the correct space group, which could have been either  $I\bar{4}3m$  or  $Im\bar{3}m$ . By comparing the values of Table 1 with those of DSSW it becomes immediately obvious that the choice for cubic CAW is definitely  $I\bar{4}3m$ , as the refined positions of O, Ca and O2 deviate significantly from the special ones required by  $Im\bar{3}m$  ( $x, x, \frac{1}{2}$ ,  $\frac{1}{4}, \frac{1}{4}, \frac{1}{4}$  and  $x, x, \frac{1}{2}$ , respectively).

The structure determinations have revealed that both cubic CAW and cubic SACR exhibit the same kind of arrangement of the tetrahedral cage anions (Fig. 1). The respective  $XO_4$  tetrahedra are oriented in such a way that one of their (local)  $\bar{4}$  axes is parallel to one of the  $\langle 100 \rangle$  directions. In addition, the tetrahedron under consideration is rotated by approximately  $45^\circ$  about

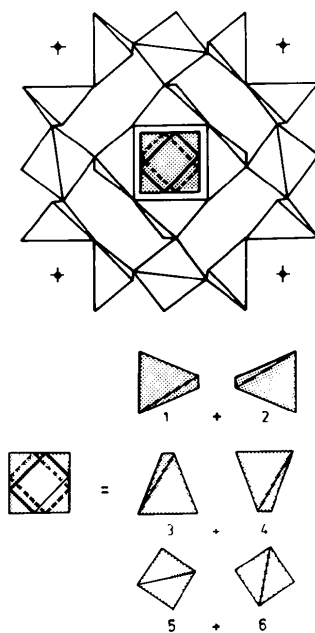


Fig. 1. One sodalite cage of cubic  $Ca_8[Al_{12}O_{24}](WO_4)_2$  projected onto (001). The unit cell is marked by crosses. Corner-connected empty tetrahedra represent the partially collapsed sodalite framework. The tilt angle is recognizable, e.g. by the deviation of certain tetrahedron edges from the cell edges ( $\sim 10^\circ$ ). The hatched distorted cuboctahedron in the centre of the sodalite cage can be thought of as being composed of six different orientation states of the disordered  $WO_4$  cage anion. These are shown in the lower part of the drawing.

this axis, in one sense or the other, out of the position in which its threefold axes coincide with those of the framework. This is the 'tetragonal orientation' mentioned earlier.\* Acting on this tetrahedron, the symmetry operations of  $I\bar{4}3m$  generate a sixfold disordered anion, whereby the  $XO_4$  O atoms are close to the diagonal mirror planes. The simplest way to mimic this type of orientational disorder crystallographically is to place this atom exactly onto the mirror plane, i.e. on  $x, x, z$ , where the O2 atom of cubic CAW has actually been found in the difference Fourier map. The 24 symmetrically equivalent positions of  $x, x, z$  (with  $x \approx 0.37$ ,  $z \approx 0.48$ ) split into two sets of twelve, each being enclosed by a sodalite cage and both isolated sets related by body centring. Each set is occupied by just one sixfold disordered  $XO_4$  group, the O2 atoms of which are at the vertices of a distorted cuboctahedron. Each of the O2 atoms belongs to two orientational states of the  $XO_4$  tetrahedron and its occupancy is, therefore,  $\frac{1}{2}$ . A stereoplot showing the disordered  $XO_4$  groups may be found in DSSW (Fig. 1). The described orientational disorder of the  $XO_4$  groups seems to be the characteristic feature of the cubic phases of aluminat sodalites.

An inspection of Tables 1 and 2 allows the following observations:

(i) The equivalent isotropic displacement parameters,  $U_{eq}$ , of cubic CAW are about five times as high as the corresponding averages of RT-CAW. This suggests that the refined  $U_{eq}$  parameters of cubic CAW can be explained only in part by the assumption of normally vibrating harmonic oscillators, since, if we accept the corresponding  $U_{eq}$  of RT-CAW as representing real thermal vibration (RT-CAW is fully ordered), then one would predict, e.g. for the  $U_{eq}$  of the tetrahedrally coordinated Al in cubic CAW, a value of about  $0.014 \text{ \AA}^2$  for an increase in temperature of about 400 K (cf. Hazen & Finger, 1982). However, the refined value is more than twice as high. Hence, an additional effect must be blamed for the difference.

(ii) Similar comments apply to the  $U_{eq}$  values of cubic SACR, which were determined at only  $\sim 40$  K above room temperature. The  $U_{eq}$  values of the framework Al and O atoms correspond to a fictitious temperature increase of about 300 K (referred to the framework of RT-CAW). The  $U_{eq}$  of the non-framework atoms have even higher values and are only slightly smaller than the corresponding values of cubic CAW.

(iii) The agreement between the refined cubic positions and the averaged orthorhombic ones is strikingly good, the difference being much smaller than the standard deviation of the orthorhombic average.

\* Locally, i.e. regarding one sodalite cage and one tetrahedral cage anion, and at a given moment, the maximal symmetry is tetragonal.

(iv) Distances and angles describing the geometry of the  $\text{AlO}_4$  tetrahedra of cubic CAW ( $l, d_1, d_2, \alpha, \alpha'$ ) correspond well to the averaged values of RT-CAW. Slightly shortened distances with respect to expected values [ $\sim 1.5\%$ , cf. Griffen & Ribbe (1979) and D2] and virtually unchanged angles are probably the manifestation of apparent bond shortening owing to increased thermal vibration [notwithstanding the additional effect mentioned in (i)].

(v) Parameters describing the degree of partial collapse of the framework ( $\gamma, u, \varphi$ ; cf. D2) are in accordance with the 1% increase of the unit-cell volume, established by the lattice-parameter determination for the two CAW phases.

(vi) A marked trend for the scatter of the  $l, d_1$  and  $u$  distances of RT-CAW is observed. The standard deviations of the average values are 0.02, 0.05 and 0.09 Å, respectively.

(vii) The distances between Ca and the framework O atoms of cubic CAW are comparable with the average Ca–O bond length of RT-CAW. On the other hand, the separation between Ca and the O2 atoms calculated for cubic CAW is clearly longer than the average bond length between the Ca and  $\text{WO}_4$  O atoms in RT-CAW.

(viii) By way of contrast, the calculated O–O2 distance in cubic CAW is significantly shorter than the average of the corresponding (short) distances in RT-CAW.

(ix) An apparent slightly shortened (1.1%) W–O2 bond length in the cubic phase can be rationalized, in the same way as under (iv), by increased thermal vibration.

Before attempting to explain the observations, a few remarks concerning the ‘tetragonal orientation’ of the cage anions  $\text{XO}_4$  and its structural consequences are necessary. In all ordered phases of aluminate sodalites known so far, the  $\text{XO}_4$  tetrahedra have been found in the ‘tetragonal orientation’. Such an arrangement results in relatively short distances between the O atoms of the  $\text{XO}_4$  groups ( $\text{O}_T$ ) and four out of twelve framework oxygens ( $\text{O}_F$ ) of the surrounding sodalite cage. These twelve  $\text{O}_F$  atoms form a (distorted) cuboctahedron [denoted 12co, cf. Figs. 7 and 8 of Koch & Hellner (1981)]. The  $\text{O}_T$ – $\text{O}_F$  distances found range from 2.9 to 3.1 Å and correspond very well to the minimum of the potential for a pair of non-bonded O atoms [cf. Fig. 4 of Hyde, Sellar & Stenberg (1986)]. The angle Al–O–Al, opening opposite to the  $\text{O}_T$ – $\text{O}_F$  interaction, is, in general, considerably enlarged with respect to the average of all angles Al–O–Al in the framework (up to  $166^\circ$  for RT-CAW, the average being  $142^\circ$ ).<sup>\*</sup> This deformation is compatible with the assumption that the  $\text{O}_F$  atoms concerned are subject to repulsion, resulting from interactions with  $\text{O}_T$  atoms.

The  $\text{O}_F$  atoms are thereby displaced to the optimum distance from  $\text{O}_T$ , corresponding to the minimum in potential energy. This group of  $\text{O}_F$  atoms will be called the ‘positive group’ ( $\text{O}_F^+$ ). To a first approximation the  $\text{O}_T$  atoms remain undisplaced, because the forces acting on the  $\text{XO}_4$  tetrahedron cancel out.

A second group of  $\text{O}_F$  atoms, called the ‘negative group’ ( $\text{O}_F^-$ ), can be distinguished. These atoms are characterized by the fact that they do not have short distances from  $\text{O}_T$  atoms, but occur together with atoms of the positive group in common four-membered rings of the sodalite framework. The corresponding Al–O–Al angles are generally reduced (down to  $128^\circ$  in RT-CAW). This reduction should be understood as being a compensation for the enlarged angles at the neighbouring  $\text{O}_F^+$  atoms. Hence, the sodalite framework is regarded as consisting of corner-sharing  $\text{AlO}_4$  tetrahedra, with common  $\text{O}_F$  atoms serving as hinges (of limited flexibility) for the otherwise quite rigid tetrahedra.

The atoms of a third group of ‘neutral’ O atoms ( $\text{O}_F^0$ ) neither have short distances from  $\text{O}_T$  atoms, nor do they share four-membered rings with  $\text{O}_F^+$  or  $\text{O}_F^-$  atoms. Their Al–O–Al angles correspond to the average of all framework atoms.

The displacements resulting from ‘positive’, ‘negative’ and ‘neutral’  $\text{O}_T$ – $\text{O}_F$  interactions must be fully coupled, such that each  $\text{O}_F^+$  compensates for an  $\text{O}_F^-$  atom, and *vice versa*. The sodalite structure is thus a typical representative of linkage structures, in which individual deviations of structural parameters from average values are compensated by others of opposite sign. The different interactions of  $\text{O}_F$  atoms with  $\text{O}_T$  atoms and the ensuing displacements result in a static distortion of the framework and, consequently, in non-cubic symmetry.

The cubic aluminate sodalites also exhibit the ‘tetragonal orientation’ of the cage anions, although disordered (see above). Whatever the actual orientation state of the  $\text{XO}_4$  tetrahedron, it must result in the described subdivision of the neighbouring  $\text{O}_F$  atoms and their corresponding displacements. Changing the tetrahedron’s orientation state also changes the framework O atoms’ classification into the different groups and their displacement. It is actually not known whether the orientational disorder of the  $\text{XO}_4$  anions is dynamic or static. However, it can surely be stated that in the cubic phases all the different ‘tetragonal orientation’ states of the  $\text{XO}_4$  tetrahedra occur with equal probability. By the various interactions between  $\text{O}_T$  and  $\text{O}_F$  atoms, the *orientational* disorder of the  $\text{XO}_4$  anions is transferred to the sodalite framework. Here it manifests itself as *positional* disorder of the Al and  $\text{O}_F$  atoms.

This view is supported by observations (i) and (ii) concerning the refined  $U_{\text{eq}}$  parameters of Al and  $\text{O}_F$  atoms in the cubic phases of CAW and SACR. These values are far too high to be accounted for by normal

<sup>\*</sup> A detailed analysis of the structure of RT-CAW is available upon request (Depmeier, 1984c,d).

thermal vibration. They must rather be regarded as the combination of a normal temperature factor and an additional term describing the positional disorder. The latter term can be estimated roughly for the Al atoms of the two cubic phases in question. In their Table 6-4, Hazen & Finger (1982) list parameters describing the variation of isotropic 'temperature factors' with temperature, including that for  $\text{Al}^{3+}$  in a tetrahedral framework. Applying the given relationship to the equivalent  $U$  values of Table 1 – and referring to RT-CAW as the ordered phase, *i.e.* subtracting the corresponding value and also accounting for the temperature of the experiment – one obtains for cubic CAW a contribution of the positional disorder to the displacement parameter of Al of  $\sim 0.017 \text{ \AA}^2$ . This value corresponds to a fictitious temperature increase of about 900 K. Similarly, the corresponding value for cubic SACR amounts to  $\sim 300 \text{ K}$ . These different results suggest that the displacements due to the repulsion between  $\text{O}_T$  and  $\text{O}_F^+$ , and the connected compensating effects on  $\text{O}_F^-$ , are much more pronounced for CAW than they are for SACR. However, this is what one would expect for an aluminate sodalite containing larger anions, but smaller cations.

The difference between both cubic phases concerning the displacement parameters of the cage anions ( $\text{WO}_4$  and  $\text{CrO}_4$ ) and cage cations (Ca and Sr), is much less marked than for the framework atoms [observation (ii)]. We believe this is the result of the essentially identical behaviour of the orientationally disordered cage anions, and of the cage cations' capability of adapting themselves relatively freely to the given circumstances, that is to follow the displacements of their coordination partners ( $\text{O}_T$  and  $\text{O}_F$ ).

Observation (iii) shows that the centres of gravity of both structures match very well. This means that the static and periodic displacements of RT-CAW have their counterpart in the non-periodic – and perhaps dynamic – displacements of cubic CAW. Furthermore, in view of the underlying mechanism, one would also expect that the extent of framework deformation should be similar for both phases. In fact, this is confirmed by the standard deviations of the mean Al and  $\text{O}_F$  positions of RT-CAW (Table 1), which, after transforming to  $\text{\AA}$  and squaring, correspond reasonably well to the  $U_{\text{eq}}$  values of cubic SACR.

Recently, it has been argued (D2) that the  $\text{AlO}_4$  tetrahedra of aluminate sodalites inherently undergo a strong angular distortion. This is confirmed by the present study. There is no substantial change in the geometry of the  $\text{AlO}_4$  tetrahedra on passing from one phase of CAW to the other [observation (iv)], the main difference being that the periodic/static distortion of RT-CAW becomes non-periodic/(perhaps) dynamic in the case of cubic CAW (see above).

Similar statements hold for the parameters describing the partial collapse of the framework [observation (v)].

The *average* conformational characteristics of the framework agree in the two phases of CAW. However, the distribution of the deviations from the average in the case of RT-CAW is highly anisotropic and becomes noticeable as non-zero values of the spontaneous deformation (Depmeier, 1988). In the cubic phase these values must be zero by symmetry and this easily measurable parameter distinguishes RT-CAW from cubic CAW.\*

The distances quoted in observation (vi) concern the Al–O bond lengths within  $\text{AlO}_4$  tetrahedra ( $l$ ), the  $\text{O}\cdots\text{O}$  distances as a measure for the angular distortion of these tetrahedra ( $d_1$ ) and the degree of partial collapse of the framework, measured by the distance between the Al atoms of neighbouring tetrahedra ( $u$ ).  $d_1$  and  $u$  have been chosen here to replace the angles  $\alpha$  and  $\gamma$ . The observed trend of increasing standard deviation in  $l$ ,  $d_1$  and  $u$  is inversely proportional to the corresponding force constants and indicates, therefore, the increasing ease of deformation of the corresponding item. The observation shows that in discussing the conformation of sodalite frameworks the bond length cannot be neglected (*cf.* Depmeier, 1984c).

The conspicuous differences between the two phases of CAW, stated in observations (vii) and (viii), are easily explained. Only the shortest distances contribute to the quoted average of the Ca–O2 and O–O2 distances in RT-CAW, whereas in the cubic phase the average is taken to include 'right' and 'wrong'  $\text{WO}_4$  tetrahedron orientations. Thereby, too long (Ca–O2) or too short (O–O2) distances are inevitably taken into account, leading to the apparently changed distances.

The value of the tilt angle of CAW ( $11.5^\circ$ ) is indicative of a fairly strong partial collapse of the framework, reflecting the small size of the Ca cation as compared with, for example, Sr in SACR, the latter having an (almost) fully expanded framework. The small size of the Ca cation also becomes noticeable in its position, which deviates significantly from  $\frac{1}{4}, \frac{1}{4}, \frac{1}{4}$ , the position of the larger Sr in SACR. Nyman & Hyde (1981) have proposed an interesting description of the cage cations in a cubic sodalite. These, being on  $x, x, x$  [ $8(c)$  in  $I43m$ ], occupy the vertices of corner-connected polyhedra which form a three-dimensional network interpenetrating the sodalite framework. With  $x = \frac{1}{4}$  the polyhedra are cubes, with  $x = 0.187$  they are ideal *stellae quadrangulae*. The actual value for cubic CAW is  $x = 0.2339$  and it is clear that the corresponding polyhedron is much more a cube rather than a *stella quadrangula*. Of course, this applies even more for cubic SACR. The mineral sodalite (Löns & Schulz, 1967) contains Na and Cl as cage ions. Na and Ca

\* In fact, the intermediate phase already exhibits an almost zero value for the spontaneous deformation, despite the fact that it is symmetry-allowed. This is a valuable clue to the particularities of this phase.

have almost the same size, but the  $x$  parameter of Na in sodalite is only 0.177. The straightforward explanation for the different shapes of the cation polyhedra is that the polyhedron 'collapses' around the relatively small  $\text{Cl}^-$  ion in the case of sodalite, whereas it is widened when it encloses the voluminous  $\text{XO}_4$  groups which are characteristic for aluminate sodalites.

In DSSW a method was proposed to describe conveniently some features of the coordination behaviour of the cage cations in the case of cubic sodalites. Thereby, planes of  $\text{O}_F$  atoms ('star', 'antistar') and of  $\text{O}_T$  atoms ('co-star', 'co-antistar'), perpendicular to [111], were considered (*cf.* Fig. 1 of DSSW). Fig. 2 shows the corresponding schematic drawing for cubic CAW which should be compared with Fig. 2 of DSSW in order to see how increasing partial collapse (CAW) changes the coordination characteristics. The essential differences can be summarized as follows:

(i) In the (almost) fully expanded state (SACR), the cage cation has (almost) equal distances from the 'star' and the 'antistar'  $\text{O}_F$  atoms. Its position is (almost) midway between the two corresponding planes.

(ii) In the partially collapsed CAW, the bonds to the  $\text{O}_F$  atoms of the 'star' are now significantly shorter than those to the 'antistar' atoms. At the same time, however, the cage cation is closer to the *plane* of the 'antistar' than to the *plane* of the 'star'. This at first sight puzzling behaviour is achieved by the cooperative rotations (tilts) of the  $\text{AlO}_4$  tetrahedra. Both 'star' and 'antistar' form equilateral triangles centred about [111]. On tilting, the 'star' atoms approach each other

(4.08 Å), whereas the 'antistar' atoms move away from each other (4.93 Å). The corresponding distances in cubic SACR are 4.52 and 4.56 Å, respectively. The values shown in Fig. 2 (and Fig. 2 of DSSW), indicate that increased tilting widens the 'antistar' triangle, whereby the bonding of the cage cation with the  $\text{O}_T$  atoms of the 'co-antistar' is favoured. This happens, however, at the expense of the bonding with the 'co-star' atoms.

### Conclusion

We believe that our analysis has revealed that disorder of all constituents of the structure is the essential feature of the cubic phases of aluminate sodalites, at least for those dealt with in this study. Orientational disorder of the cage anions is thereby transferred to the framework as well as to the cage cations, where it manifests itself as positional disorder. The differences between the orthorhombic and cubic phases of CAW indicate that periodic and static atomic displacements from average positions in the former case become non-periodic in the latter. Until now it has not been known whether the disorder in the cubic phases is static or dynamic in nature, as our elastic scattering experiments were not sensitive to this difference. We hope, however, that future experiments, using different techniques, will help to elucidate this point.

It is a pleasure to thank Professor H. Bärnighausen for making available the crystal heater and Mrs H. Schnittka for the drawings.

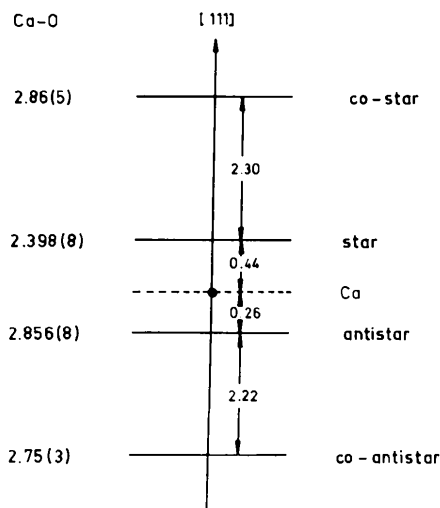


Fig. 2. Coordination characteristics along [111] for Ca in cubic  $\text{Ca}_8[\text{Al}_{12}\text{O}_{24}](\text{WO}_4)_2$ . Ca-O distances are given on the left, distances between planes on the right-hand side. All distances are in Å. 'Star' and 'antistar' are planes within the sodalite framework, whereas 'co-star' and 'co-antistar' form part of two disordered  $\text{WO}_4$  groups situated in two adjacent sodalite cages. This drawing should be compared with Fig. 2 of Depmeier, Schmid, Setter & Werk (1987).

### References

- ANSELMET, B. (1986). *Die Dynamik der Phasenumwandlung vom Rutil- in den  $\text{CaCl}_2$ -Typ am Beispiel des  $\text{CaBr}_2$  und zur Polymorphie des  $\text{CaCl}_2$* . Dissertation, Univ. Karlsruhe (TH), Federal Republic of Germany.
- DEPMEIER, W. (1979). *J. Appl. Cryst.* **12**, 623–626.
- DEPMEIER, W. (1984a). *Acta Cryst.* **C40**, 226–231.
- DEPMEIER, W. (1984b). *Acta Cryst.* **B40**, 185–191.
- DEPMEIER, W. (1984c). *Description and Discussion of the Anisotropically Folded Aluminate Sodalite  $\text{Ca}_8[\text{Al}_{12}\text{O}_{24}](\text{WO}_4)_2$ . I. The Sodalite Framework*. Unpublished.
- DEPMEIER, W. (1984d). *Description and Discussion of the Anisotropically Folded Aluminate Sodalite  $\text{Ca}_8[\text{Al}_{12}\text{O}_{14}](\text{WO}_4)_2$ . II. The Cage Contents*. Unpublished.
- DEPMEIER, W. (1988). *Phys. Chem. Miner.* Submitted.
- DEPMEIER, W., SCHMID, H., SETTER, N. & WERK, M. (1987). *Acta Cryst.* **C43**, 2251–2255.
- GRIFFEN, D. T. & RIBBE, P. H. (1979). *Neues Jahrb. Mineral. Abh.* **137**, 54–73.
- HASSAN, I. & GRUNDY, H. D. (1984). *Acta Cryst.* **B40**, 6–13.
- HAZEN, R. M. & FINGER, L. W. (1982). *Comparative Crystal Chemistry*. New York: John Wiley.
- HYDE, B. G., SELLAR, J. R. & STENBERG, L. (1986). *Acta Cryst.* **B42**, 423–429.
- International Tables for X-ray Crystallography* (1974). Vol. IV. Birmingham: Kynoch Press. (Present distributor D. Reidel, Dordrecht.)
- KOCH, E. & HELLNER, E. (1981). *Z. Kristallogr.* **154**, 95–114.

LÖNS, J. & SCHULZ, H. (1967). *Acta Cryst.* **23**, 434–436.  
 NYMAN, H. & HYDE, B. G. (1981). *Acta Cryst.* **A37**, 11–17.  
 ROGERS, D. (1981). *Acta Cryst.* **A37**, 734–741.  
 SETTER, N. & DEPMEIER, W. (1984). *Ferroelectrics*, **56**, 45–48.

SHELDRIK, G. M. (1978). *SHELXTL. An Integrated System for Solving, Refining and Displaying Crystal Structures from Diffraction Data*. Univ. of Göttingen, Federal Republic of Germany.

*Acta Cryst.* (1988). **B44**, 207–227

## The Structure of $\{111\}$ Age-Hardening Precipitates in Al–Cu–Mg–Ag Alloys

BY K. M. KNOWLES AND W. M. STOBBS

*University of Cambridge, Department of Materials Science and Metallurgy, Pembroke Street, Cambridge CB2 3QZ, England*

(Received 28 July 1987; accepted 9 December 1987)

### Abstract

High-resolution transmission electron microscopy (HREM) of  $\{111\}$  precipitates in an Al–Cu–Mg–Ag alloy has been used to confirm by direct observation down  $\langle 110 \rangle$  and  $\langle 211 \rangle$  Al matrix zone axes that the structure of these precipitates in peak- and over-aged material is consistent with the monoclinic structure proposed by Auld [*Acta Cryst.* (1972), **A28**, S98] of  $a = b = 4.96$ ,  $c = 8.48$  Å,  $\gamma = 120^\circ$ , rather than the hexagonal structure with  $a = 4.96$ ,  $c = 7.01$  Å proposed by Kerry & Scott [*Met. Sci.* (1984), **18**, 289–294]. Reexamination of the monoclinic structure suggested by Auld shows that the structure he proposes is in fact orthorhombic ( $a = 4.96$ ,  $b = 8.59$ ,  $c = 8.48$  Å), and is best regarded as a distortion of the structure of tetragonal  $\theta$ -Al<sub>2</sub>Cu precipitates found in over-aged Al–Cu alloys. A detailed reanalysis of electron diffraction patterns from this alloy in the light of HREM observations confirms that this structure and the relative thinness of these precipitates perpendicular to the  $\{111\}$  planes can indeed together satisfactorily account for the extra spots and streaks in the patterns.

### 1. Introduction

Suitable heat treatments of Al–Cu–Mg alloys with high Cu:Mg ratios and trace additions of silver can cause precipitates to nucleate and grow on  $\{111\}$  planes as well as  $\{100\}$  planes of the aluminium matrix (Taylor, Parker & Polmear, 1978; Chester & Polmear, 1983), and the occurrence of these thin disc-like precipitates significantly enhances the age-hardening characteristics of such alloys. The composition range within which these  $\{111\}$  precipitates have been found to occur suggests that they should be formed in the commercial Al–Cu–Mg–Ag alloys 201 and Avoir under suitable heat treatments, and indeed castings from such alloys are noted for their marked response to age hardening and for their good tensile properties (Iler,

1969; Taylor, Parker & Polmear, 1978). More recently, Brown Boveri have developed an experimental Al–Cu–Mg–Ag–Mn–Zr–Ti alloy for improved high-temperature strength and creep resistance, and the superior properties of this alloy over 2618 and 2219 arise from a fine dispersion of these  $\{111\}$  precipitates (Kubel, 1986; Polmear, 1986). It is therefore of interest to determine why it is energetically favourable for the  $\{111\}$  precipitates to form in these alloys and, from a knowledge of their structure and chemical composition, to determine whether such precipitates can be expected to occur in other aluminium alloy systems.

The role of the silver and the requirements of a high Cu:Mg ratio (Chester & Polmear, 1983) in promoting the  $\{111\}$  precipitation is as yet unclear. Taylor, Parker & Polmear (1978) suggested that the precipitates nucleate as Mg<sub>3</sub>Ag, before growing and attaining an overall composition close to Al<sub>2</sub>Cu. However, in agreement with the earlier work of Williams (1972), a recent study of precipitation processes in Al-rich Al–Mg–Ag alloys by Cousland & Tate (1986) has failed to isolate Mg<sub>3</sub>Ag as a precipitating phase in ternary alloys, even in alloys with a high Mg to Ag ratio. Instead, Cousland & Tate showed that the phases that they observed containing only Ag and Mg atoms were of composition MgAg (their type 1 and type 2 GP zones). This would suggest that the nucleation mechanism for the  $\{111\}$  precipitates suggested by Taylor, Parker & Polmear (1978) is unlikely.

Furthermore, the structure of these precipitates is still a matter of debate. Auld (1972, 1986) has proposed a monoclinic unit cell on the basis of X-ray evidence with  $a = b = 4.96$ ,  $c = 8.48$  Å and  $\gamma = 120^\circ$ , and showed that this structure can be considered to be a slightly distorted form of the structure of the incoherent  $\theta$ -Al<sub>2</sub>Cu precipitates (Guinier, 1942; Silcock, Heal & Hardy, 1953–1954; Laird & Aaronson, 1966). In contrast to this, Kerry & Scott (1984) have proposed a hexagonal unit cell with  $a = 4.96$  and  $c = 7.01$  Å from their analysis of electron diffraction patterns of peak-